



## ORIGINAL ARTICLE

# Synthesis and characterization of surfactant assisted $Mn^{2+}$ doped ZnO nanocrystals



N. Shanmugam \*, K. Dhanaraj, G. Viruthagiri, K. Balamurugan, K. Deivam

Department of Physics, Annamalai University, Chidambaram, India

Received 5 May 2011; accepted 20 August 2011

Available online 27 August 2011

## KEYWORDS

Zinc oxide;  
PVP;  
Quantum confinement;  
Agglomeration;  
Nanorod

**Abstract** We report the synthesis and characterization of Mn doped ZnO nanocrystals, both in the free standing and PVP capped particle forms. The nanocrystals size could be controlled by capping them with polyvinylpyrrolidone and was estimated by X-ray diffraction and transmission electron microscopy. The chemical compositions of the products were characterized by FT-IR spectroscopy. UV–Vis absorption spectroscopy measurements reveal that the capping of ZnO leads to blue shift due to quantum confinement effect. The morphology of the particles was evaluated by Scanning Electron Microscopy (SEM) and Transmission Electron Microscopy (TEM). Both the Thermo Gravimetric Analysis (TGA) and Differential Thermal Analysis (DTA) curves of the ZnO show no further weight loss and thermal effect at a temperature above 510 °C.

© 2011 Production and hosting by Elsevier B.V. on behalf of King Saud University. This is an open access article under the CC BY-NC-ND license (<http://creativecommons.org/licenses/by-nc-nd/3.0/>).

## 1. Introduction

In the present trend, Zinc Oxide, a wide band gap ( $E_g \sim 3.37$  eV) II–VI semiconductor has been playing a vital role because of its application in UV light-emitters, varistors, surface acoustic wave devices, piezo electric transducers, gas sensors and solar cells (Zu et al., 1997; Tang et al., 1998; Jin et al., 2000; Look, 2001). The optical properties of nanomaterials differ from those in the bulk materials due to quantum confinement effects (Tao et al., 2008). To promote the forma-

tion of ZnO nanostructures poly-vinylpyrrolidone (PVP) is frequently used as a templating molecule (Lepton et al., 2007). Despite, a variety of techniques have been employed for the synthesis of ZnO particles, such as sol-gel (Vayssieres et al., 2001), hydrothermal (Hu et al., 2002), chemical vapour deposition (CVD) (Wu and Sai-Chang, 2002), electrophoretic deposition (Yang, 2003), vapour–liquid–solid (VLS) method (Huang et al., 2001; Yang et al., 2002), and thermal decomposition (Yin et al., 2004), the above routes need high temperature, high pressure and expensive raw materials, which constrained that they are not suitable for large scale production with a relatively low cost. In this paper we report the synthesis and characterization of Mn doped ZnO nanocrystals via simple chemical precipitation method. To control the size and shape of the particles, we have capped Mn doped ZnO nanocrystals with polyvinylpyrrolidone (PVP). The prepared nanocrystals are characterized using X-ray Diffractometer (XRD), Fourier Transform Infra Red (FTIR) spectroscopy, Scanning

\* Corresponding author. Tel.: +91 9444276357.

E-mail address: [quantumgosh@rediffmail.com](mailto:quantumgosh@rediffmail.com) (N. Shanmugam).

Peer review under responsibility of King Saud University.



Production and hosting by Elsevier

Electron Microscopy (SEM), Transition Electron Microscopy (TEM), UV-Visible absorption spectra, and Thermo Gravitric-Differential Thermal analysis (TG-DT).

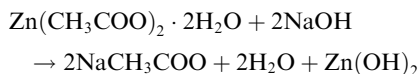
## 2. Experimental

### 2.1. Materials

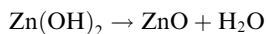
Zinc acetate dihydrate (Zn(CH<sub>3</sub>COO)<sub>2</sub>·2H<sub>2</sub>O), sodium hydroxide (NaOH), manganese chloride (MnCl<sub>2</sub>·4H<sub>2</sub>O), and poly-vinylpyrrolidone (PVP mw = 40,000) were used as received to prepare Mn doped ZnO, and PVP encapsulated Mn doped ZnO nanocrystals. Throughout the process deionized water was used as solvent.

### 2.2. Synthesis of ZnO nanocrystals

In the synthesis of ZnO nanoparticles 2.2 g of Zinc acetate was dissolved in 100 ml of deionized water and then stirred the solution vigorously by a magnetic stirrer. Next the solution of 0.05 g of NaOH in 100 ml of deionized water was added drop wise to zinc acetate solution under vigorous stirring. By gradually mixing the solution of Zn(CH<sub>3</sub>COO)<sub>2</sub>·2H<sub>2</sub>O and NaOH a white precipitate of Zn(OH)<sub>2</sub> nanoparticles was formed. The overall reaction for the synthesis of ZnO can be written as



The precipitate was collected and rinsed three times with high purity water and ethanol, respectively. Subsequently, the washed precipitate was dried at 100 °C for 2 h to form the precursor ZnO.



### 2.3. Synthesis of PVP encapsulated ZnO nanocrystals

For the synthesis of PVP encapsulated ZnO, 1 g of PVP dissolved in 100 ml of deionized water was mixed with Zinc acetate solution (2.2 g in 100 ml of DIW). After several mixing, the aqueous solution of NaOH (0.05 g in 100 ml of DIW) was added drop wise under vigorous stirring to form white precipitate of PVP encapsulated ZnO nanocrystals.

### 2.4. Synthesis of PVP encapsulated ZnO:Mn<sup>2+</sup>

For the synthesis of PVP encapsulated ZnO:Mn<sup>2+</sup>, 1 g of PVP dissolved in 100 ml of deionized water was mixed with zinc acetate solution (2.2 g in 100 ml of DIW). After several mixing, the aqueous solutions of MnCl<sub>2</sub>·4H<sub>2</sub>O (6 wt %) and NaOH (0.05 g in 100 ml of DIW) were added drop wise under vigorous stirring to form white precipitate of PVP encapsulated ZnO:Mn<sup>2+</sup>.

### 2.5. Characterization techniques

X-ray diffraction patterns of the ZnO, Mn doped ZnO and PVP encapsulated ZnO:Mn<sup>2+</sup> were recorded using an XPERT-PRO diffractometer with a CuK $\alpha$  radiation ( $\lambda = 1.54060 \text{ \AA}$ ) under the same conditions. The crystallite size

was calculated using Debye-Scherer equation  $D = 0.89 \lambda / \beta \cos \theta$  using the half width at full maximum of the major XRD peaks. The FT-IR studies were carried out using NICO-LET AVATAR 360 FT-IR spectrometer. The optical absorption spectra of the samples were recorded using a UV 1650 PCSHIMADZU spectrometer. Size and morphology of the particles were determined using TEM (PHILIPS-CM200; 20–20 kv) and Scanning Electron Microscopy (SEM; JEOL-JSM-5610LV). Elemental composition was analysed using the EDX attachment to the SEM. Thermo Gravimetric-Differential Thermal Analysis was carried out by STD Q600V 8.3 Build 101 thermal analyzer under nitrogen atmosphere at the rate of 10 °C/min.

## 3. Results and discussion

### 3.1. Crystal structure analysis and determination of crystallite size

The XRD patterns of undoped ZnO, Mn<sup>2+</sup> doped ZnO and PVP encapsulated ZnO:Mn<sup>2+</sup> nanoparticles are shown in Fig. 1. All the diffraction peaks exhibit the typical ZnO wurtzite hexagonal structure (Sharda et al., 2010). Diffraction peaks related to impurities were not observed in the XRD pattern, confirming the high purity of the synthesized products. Furthermore, it could be noted that the diffraction peaks of ZnO:Mn<sup>2+</sup> and PVP encapsulated ZnO:Mn<sup>2+</sup> nanoparticles were more intense and sharper implying a good crystalline nature of the as synthesized ZnO products (Rajeswari Yogamalar et al., 2009). In addition, the broadening of the diffraction peaks also denotes that the crystallite sizes were small as a result of Mn doping and PVP capping. The average crystallite size (*D*) of the nanosized particles can be obtained from Debye-Scherrer formula  $D = 0.89\lambda / (\beta \cos \theta)$ , where *D* is the crystallite size (in nm),  $\beta$  the full width at half maximum (FWHM – in radians), and  $\theta$  the Bragg diffraction angle. The average crystallite size was estimated as 12.5, 10.5 and 8.5 nm for undoped ZnO, Mn<sup>2+</sup> doped ZnO and PVP encapsulated ZnO:Mn<sup>2+</sup>, respectively. These results show that PVP plays an important role in controlling the ZnO particles size.

### 3.2. Functional group analysis

The presence of various chemical functional groups and the formation of ZnO nanoparticles are supported by FT-IR spectra as shown in Fig. 2. The broad absorption bands at 3434 and 1636 cm<sup>-1</sup> are due to O–H stretching and bending vibrations of absorbed water at the surface of particles. The absorption peak around 2432 cm<sup>-1</sup> is due to the existence of CO<sub>2</sub> molecules in air. The strong absorption bands between 550 and 430 cm<sup>-1</sup> can be attributed to the stretching modes of ZnO (Fernandes et al., 2009). The appearance of the absorption band at 464 cm<sup>-1</sup> explains the morphology dependency of the synthesized ZnO particles as spherical (The Infrared Spectra Hand book of Inorganic Compounds, 1984). The spectra obtained for uncapped and capped ZnO:Mn<sup>2+</sup> particles are more or less similar. The recorded peaks between 1600 and 1400 cm<sup>-1</sup> correspond to the asymmetric and symmetric stretching of the carboxyl group (C=O). The peak around 620 cm<sup>-1</sup> corresponds to the bending vibration of Mn. However, in the capped ZnO:Mn<sup>2+</sup> few additional peaks at

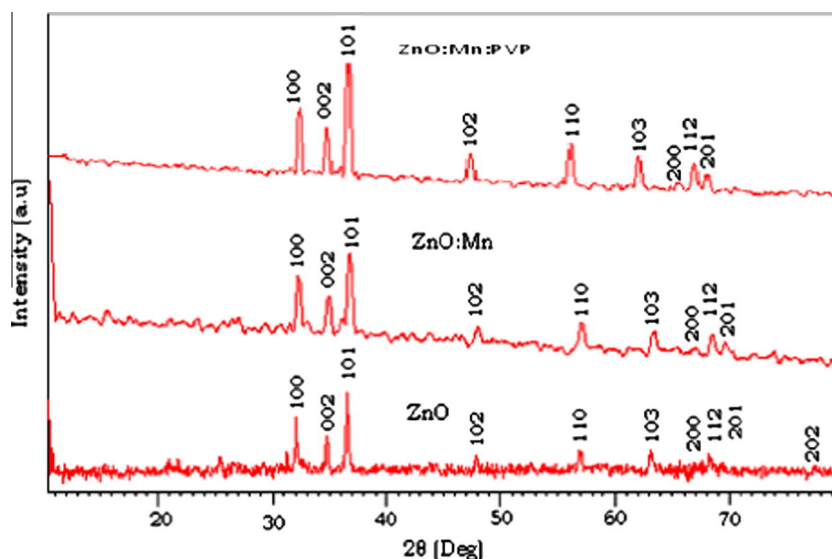


**Figure 1** XRD patterns of undoped ZnO, ZnO:Mn<sup>2+</sup> and PVP capped ZnO, ZnO:Mn<sup>2+</sup> nanoparticles.

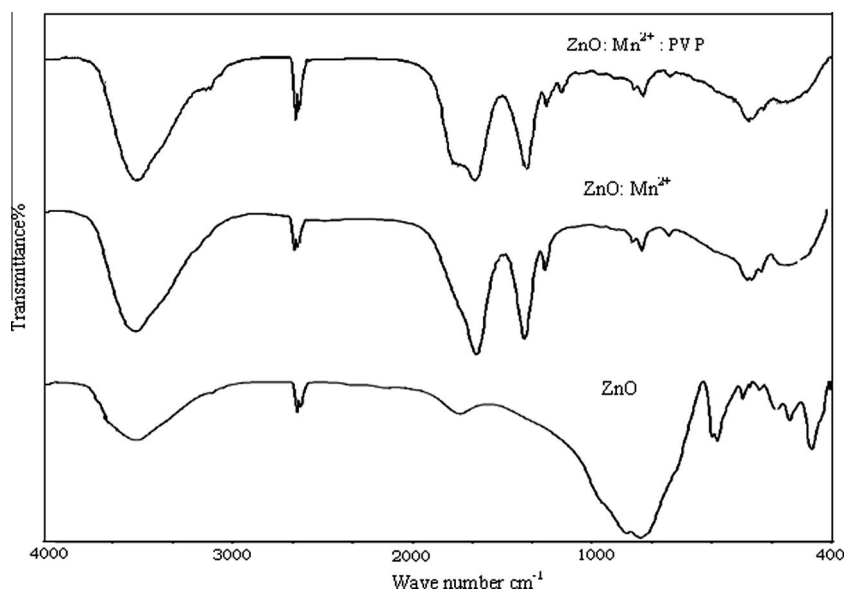


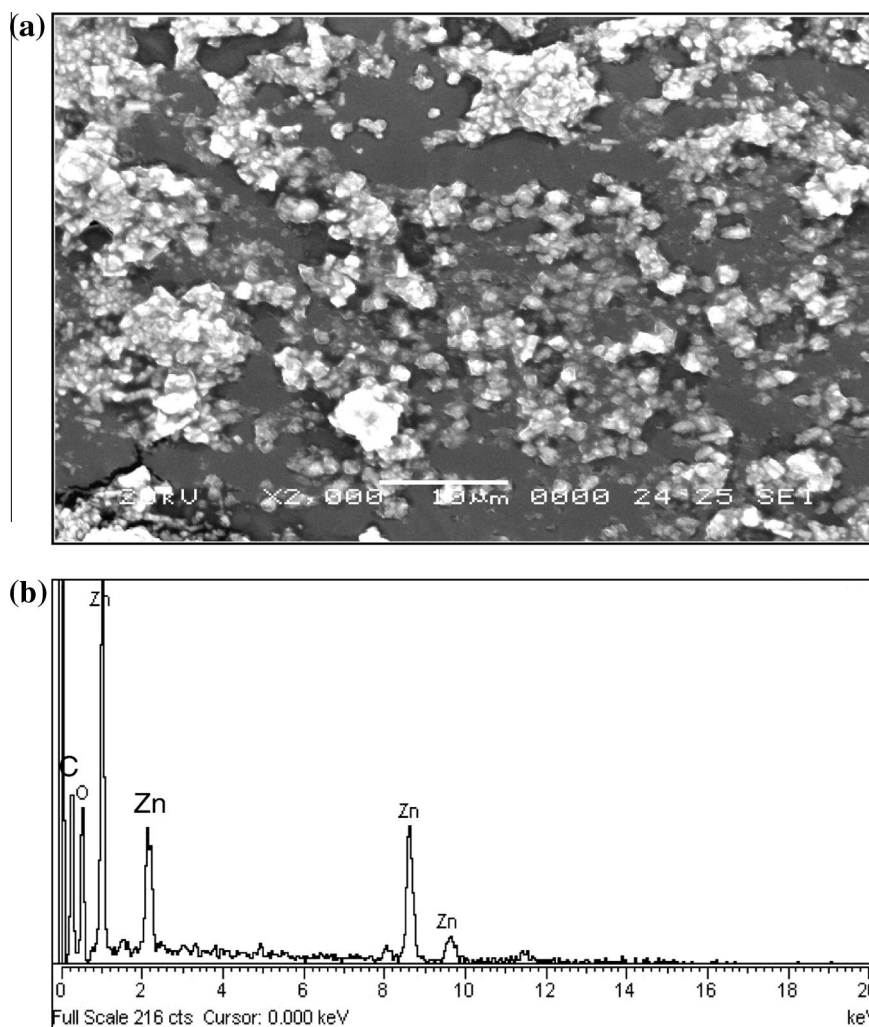
**Figure 2** FT-IR spectra of ZnO, ZnO:Mn<sup>2+</sup> and PVP encapsulated ZnO:Mn<sup>2+</sup>.

2953, 1647 and 1293  $\text{cm}^{-1}$  are assigned to the  $\text{CH}_2$  asymmetrical stretching vibration, bending vibration of polymeric network and C–N stretching vibration, respectively. The appearance of large number of IR bending modes for capped particles indicates the formation of smaller sized particles when compared with the uncapped particles. The intensity of the IR peaks for PVP capped ZnO:Mn<sup>2+</sup> is higher than that of uncapped nanoparticles, which indicates the homogeneous formation of particles.

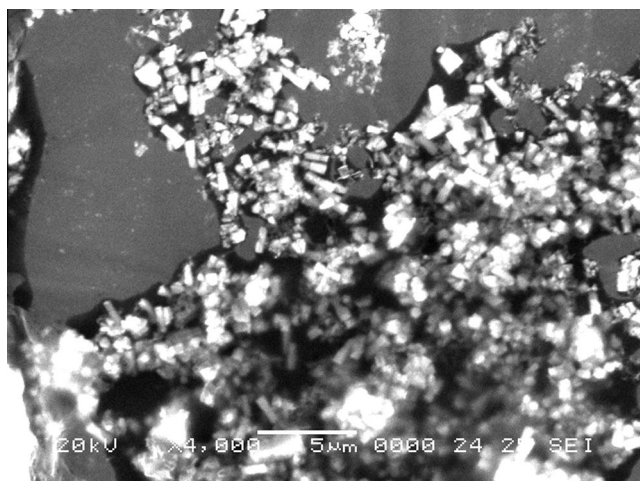
### 3.3. Particles morphology

Fig. 3a shows the SEM image of undoped ZnO particles and the corresponding EDX is given in Fig. 3b. SEM image reveals that the particles are spherical in shape and monodispersed

with the size less than 100 nm. The EDX spectrum confirms the composition of ZnO. The SEM image of Mn doped ZnO is shown in Fig. 4. It clearly indicates that the transformation of spherical particles into rod shape with particle size confinement as a result of Mn doping. Fig. 5a shows the SEM image of PVP encapsulated ZnO:Mn<sup>2+</sup> nanoparticles, which indicates that the rod like structure of nanoparticles accompany with spherical particles. It was also found that the capped ZnO nanoparticles have better morphology than that of the uncapped one. The results demonstrate that the PVP plays an important role in controlling the size and shape of ZnO particles. PVP acts as a template, which can form chain structures. With the polymer template, ZnO can grow up along these chains to form nanostructure. On the other hand, PVP can form a shell surrounding the particles to prevent them from



**Figure 3** SEM image of undoped ZnO nano particles (a) and corresponding EDX spectrum (b).



**Figure 4** SEM image of  $\text{Mn}^{2+}$  doped ZnO nanoparticles.

agglomeration to larger particles as a result of its steric effect. (Bai et al., 2005). The EDX pattern of capped  $\text{ZnO}:\text{Mn}^{2+}$  is shown in Fig. 5b that confirms the incorporation of Mn.

The TEM images of ZnO and PVP capped  $\text{ZnO}:\text{Mn}^{2+}$  are shown in Figs. 6 and 7. It is clear that in the prepared ZnO powders many of them tend to agglomerate which indicates the incomplete nucleation growth. In the TEM image of PVP coated  $\text{ZnO}:\text{Mn}^{2+}$  the particles are well separated with no agglomeration. With the introduction of PVP, Zinc ions or particles would coordinate with N or O in PVP, and a covered layer would generate on the surface of the particles. The layer inhibited the growth and agglomeration of the particles. As can be seen from Fig. 7, the sample consists of straight and smooth rods. The diameter and the length of the nanorods are in the range of 9–12.5 and 52–100 nm, respectively. These results are in good agreement with the values obtained by XRD data mentioned above.

#### 3.4. Optical absorption

Fig. 8 shows the absorption spectra of undoped ZnO,  $\text{Mn}^{2+}$  doped ZnO and PVP capped  $\text{ZnO}:\text{Mn}^{2+}$  nanoparticles. The absorption peaks corresponding to ZnO,  $\text{ZnO}:\text{Mn}^{2+}$  and PVP capped  $\text{ZnO}:\text{Mn}^{2+}$ , are 345, 334 and 325 nm, respectively and the peak position reflects the band gap of the nanoparticles. Compared to ZnO nanoparticles, PVP encapsulated

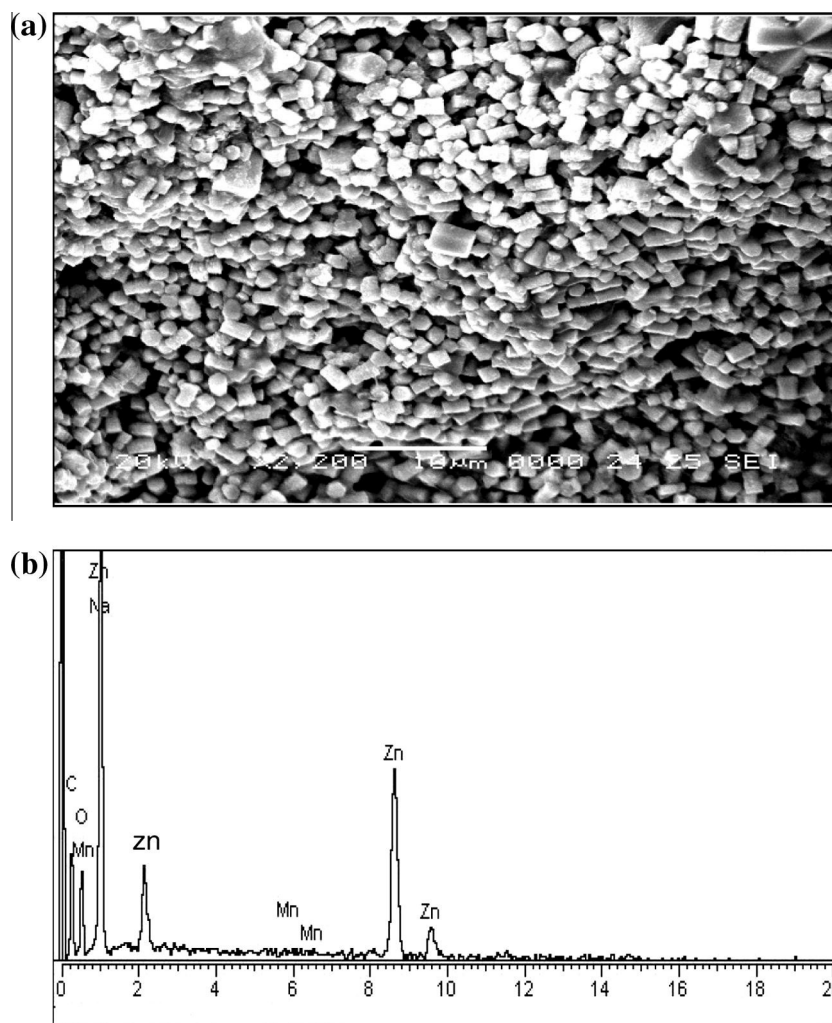


Figure 5 SEM image of PVP encapsulated  $\text{ZnO:Mn}^{2+}$  (a) and corresponding EDX spectrum (b).



Figure 6 TEM image of ZnO nanoparticles.

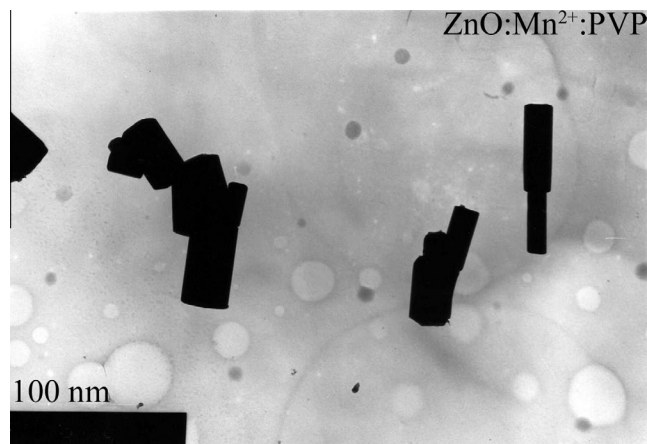
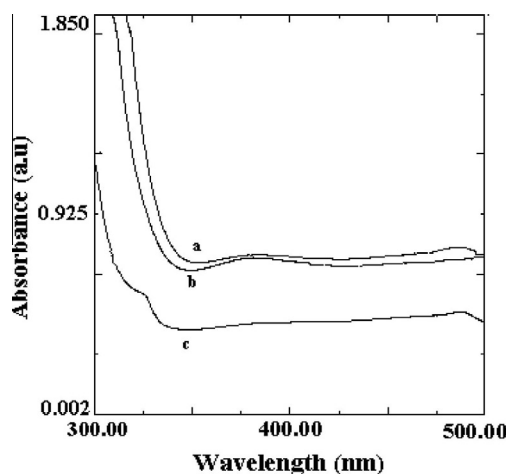


Figure 7 TEM image of PVP encapsulated  $\text{ZnO:Mn}^{2+}$ .

$\text{ZnO:Mn}$  nanoparticles have significant blue-shifted absorption peak due to the controlled growth of the ZnO shell on  $\text{ZnO:Mn}$  core particles. The optical band gaps were calculated and are 3.60, 3.71 and 3.82 eV, respectively, for undoped ZnO,  $\text{ZnO:Mn}^{2+}$  and PVP encapsulated  $\text{ZnO:Mn}^{2+}$  nanoparticles.

The obtained values of the band gap of the synthesized nanoparticles are higher than those of the bulk value of ZnO (3.37 eV). This blue shift of the band gap takes place because of the quantum confinement effect (Bhargava and Gallagher, 1994).



**Figure 8** Absorption spectra of ZnO (a)  $\text{ZnO:Mn}^{2+}$  (b) and PVP encapsulated  $\text{ZnO:Mn}^{2+}$  (c) nanoparticles.

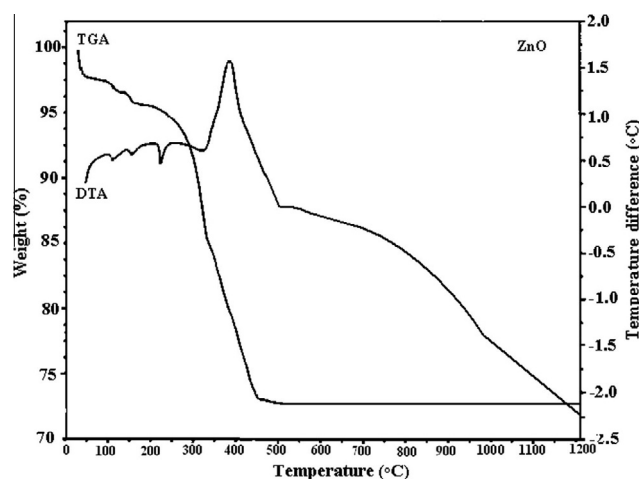


**Figure 9** TG-DTA curve of the prepared ZnO nano crystals.

### 3.5. Thermal analysis of ZnO

Fig. 9 shows the TG and DTA traces of ZnO which was heated from room temperature to 1200 °C at 10 °C/min under a nitrogen atmosphere. TGA curve shows that the major weight loss occurs in the temperature range of 250–450 °C. The weight loss was related to the decomposition of the precursors of ZnO. The sharp plateau formed at a temperature between 450 and 1200 °C on the TGA curve indicates the formation of nanocrystalline ZnO, as confirmed by XRD analysis (Santi Maensiri et al., 2006). On the DTA curve a major exothermic peak was observed between 320 and 500 °C with a maximum at about 385 °C, indicating that the thermal event could be associated with the decomposition of the precursors of ZnO. Further more no weight loss and no thermal effect were observed for temperatures above 510 °C, indicating that decomposition does not occur above this temperature and that the stable residues may be ascribed to ZnO nanoparticles.

## 4. Conclusions

We have synthesized nanocrystals of pure, transition metal ion  $\text{Mn}^{2+}$  doped and PVP encapsulated  $\text{Mn}^{2+}$  doped ZnO through chemical precipitation method. XRD analysis revealed the formation of a single phase with a wurtzite ZnO structure and their nanocrystalline nature. The Scherrer's formula showed that the particle sizes are in the range of 12.5 nm for undoped, 10.5 nm for doped and 8.5 nm for capped nanoparticles. The FT-IR analysis has confirmed the formation of ZnO and Mn doped ZnO. SEM studies showed the transformation of spherical particles into rod shape after Mn doping and PVP capping. It was found that after capping ZnO nanoparticles have better morphology than the uncapped one and also PVP encapsulation on  $\text{ZnO:Mn}^{2+}$  decreases the size of the particles. TEM study showed that the synthesized nanorods are perfectly monodispersed. The diameter and the length of the nanorods are 9–12.5 and 52–100 nm, respectively. The optical absorption showed that UV absorption peaks of the doped and capped ZnO were blue shifted compared with bulk ZnO, which clearly indicate the strong quantum confinement. Thermal studies revealed that nanocrystalline ZnO particles are formed at the calcinations temperature of 510 °C.

## Acknowledgements

The authors wish to thank Dr. AN. Kannappan, Dean, Faculty of Science, Dr. C. Karunakaran, Professor and Head, Department of Chemistry, and Dr. S.T. Balasubramaniam, Director CAS in Marine Biology, Annamalai University, for their stimulating discussions during the period of this work.

## References

- Bhargava, R.N., Gallagher, D., 1994. Phys. Rev. Lett. 72, 416–419.
- Bai, Fanfei, He, Ping, Jia, Zhijie, Huang, Xintang, He, Yun, 2005. Mater. Lett. 59, 1687–1690.
- Fernandes, D.M., Silva, R., Winkler Hechenleither, A.A., et al., 2009. Mater. Chem. Phys. 115, 110–115.
- Hu, J.Q., Li, Q., Wong, N.B., Lee, C.S., 2002. Synthesis of uniform hexagonal prismatic ZnO Wiskers. Chem. Mater. 14, 1216–1219.
- Huang, M.H., Mao, M., Yan, H., Wu, Y., Feick, H., Russo, R., Yang, P., 2001. Room-Temperature Ultraviolet nanowire nanolasers. Science 292, 1897–1899.
- Jin, B.J., Bae, S.H., Lee, S.Y., Im, S., 2000. Mater. Sci. Eng. B 71, 301–306.
- Lepton, N., Van Bael, M.k., Van den Rul, H., D' Haen, J., Peeters, R., Franco, D., Mullens, 2007. J. Mater. Lett. 61, 2624–2627.
- Look, D.C., 2001. Mater. Sci. Eng. B 80, 383–389.
- Rajeswari Yogamalar, N., Srinivasan, R., Chandra Bose, A., 2009. Opt. Mater. 31, 1570–1574.
- Santi Maensiri, A., Paveena Laokul, R., Vinich Promarak, T., 2006. J. Crystal Growth 289, 102–106.
- Sharda, K., Jayanthi, Santa Chawla, 2010. Appl. Surface Science 256, 2630–2635.
- Tang, Z.K., Wong, G.K.L., Yu, P., Kawasaki, M., Ohtomo, A., Koinuma, H., Segawa, Y., 1998. Appl. Phys. Lett. 72, 3270–3277.
- Tao, T., Yu, X., Fei, X., Liu, J., Yang, G., Zhao, Y., Yang, S., Yang, L., 2008. Opt. Mater. 31, 1–7.
- The Infrared Spectra Hand book of Inorganic Compounds, Sadtler Research Lab (Heydens Son Ltd.; London 1984).

- Vayssieres, L., Keis, K., Hagfeldt, A., Lindquist, S.E., 2001. Three-dimensional array of highly oriented Crystalline ZnO microtubes. *Chem. Mater.* 13, 4395–4401.
- Wu, J.J., Sai-Chang, L., 2002. Growth and characterization of ZnO nanorods. *J. Phys. Chem. B* 106, 9546–9552.
- Yang, P., Yan, H., Mao, S., Russo, R., Jhonson, J., Morris, N., Pham, J., He, R., Choi, H., 2002. Controlled Growth of ZnO nanowire. *Adv. Funct. Matter.* 12 (5), 323–328.
- Yang, S.H., 2003. Electrophoretic prepared ZnGa<sub>2</sub>O<sub>4</sub> phosphor film for FED. *J. Electrochem. Soc.* 150, 250–253.
- Yin, M., Gu, Y., Kuskovsky, I.L., Andelman, T., Zhu, Y., Neumark, T.F., O'Brien, S., 2004. Zinc oxide Quantum F rods. *J. Am. Chem. Soc.* 126, 6206–6208.
- Zu, P., Tang, Z.K., Wong, G.K.L., Kawasaki, M., Ohtomo, A., Koinuma, H., Segawa, 1997. *Solid State Commun.* 103, 459–464.